Title

Solution of the infrared tomography inverse problem

ISBN

9780819420558

Authors

Smithies, Derek J
Milner, Thomas E
Nelson, J Stuart
et al.

Publication Date

1996-05-07

DOI

10.1117/12.239556

Solution of the infrared tomography inverse problem

Derek J. Smithies, Thomas E. Milner, J. Stuart Nelson

Beckman Laser Institute and Medical Clinic,
University of California Irvine, Irvine, CA 92715

Dennis M. Goodman

Lawrence Livermore National Laboratory,
University of California Livermore, Livermore, CA 94550

ABSTRACT

Infrared tomography (IRT) is a non contact method to determine the size and position of port wine stain blood vessels from analysis of recorded infrared emission images immediately following pulsed laser irradiation. To develop a diagnostic tool for clinical use, infrared emission images from laser irradiated tissue have been simulated on a computer. Analysis of the simulated infrared emission images shows that size and position of the laser heated vessels can be predicted.

Keywords: three-dimensional, computer simulation, infrared focal plane array, port wine stain

1 INTRODUCTION

Port wine stains (PWS) are congenital hypervascular cutaneous malformations that appear as a light red to purple discoloration of human skin.[1] Irradiation with a flashlamp pumped pulsed dye laser ($\lambda = 585$ nm, pulse duration $\tau_p = 450\,\mu$s) has become the treatment of choice, however, some patients experience a poor clinical result with sub-optimal fading. Several reasons for the poor response have been proposed. Tan *et al.*[2] suggest that laser wavelength should be adjusted to maximize the depth of damaged vessels. Alternatively, theoretical[3,4] and clinical studies[5] suggest the ideal pulse duration is between 0.5 and 10 ms, and depends on vessel diameter. Knowledge of vessel size and position prior to laser therapy can guide the clinician to select the appropriate pulse duration and wavelength for optimal treatment results.

The traditional method to determine PWS vessel diameter is analysis of a biopsy specimen using light microscopy. This technique is invasive and invariably leaves a scar. Furthermore, results are of questionable practical value as artifacts may be introduced during processing of the tissue specimen.

Infrared tomography (IRT)[6,7] uses a fast infrared focal plane array (IR-FPA) camera system to measure increases in infrared emission at the skin surface following pulsed laser irradiation. From the recorded time sequence of infrared emission images, size and position of subsurface chromophores can be deduced.

A mathematical relationship between the time sequence of infrared emission images and the temperature distribution within the skin immediately following pulsed laser irradiation is defined. Using this relationship, the size and position of three vessels in our model of skin is correctly estimated from a simulated time sequence of infrared emission images.

2 THEORY

The measured change in infrared emission at the the tissue surface ($\Delta M(x,y,t)$) following pulsed laser irradiation is given by,[7]

$$\Delta M(x,y,t) = \int_\xi \int_\eta \int_\zeta K_T(x-\xi, y-\eta, \zeta, t)\Delta T^{3D}(\xi,\eta,\zeta;t_o)d\xi d\eta d\zeta \tag{1}$$

0-8194-2055-7/96/$6.00

where ΔT^{3D} is the three-dimensional temperature increase in skin at the end of the laser pulse ($t = t_o$). The three-dimenensional thermal point spread function, K_T,[6,7] is an analytical expression derived from solution of the bioheat equation.[8] Lateral dimensions x and y refer to position on a plane parallel with the surface, while z is distance into the tissue from the surface ($z = 0$).

The three-dimensional thermal point spread function is dependent on tissue parameters in Table 1.

physical parameter	value
thermal diffusivity	$0.11\,mm^2 s^{-1}$
thermal conductivity	$0.005\,W\,m^{-1}\,°C^{-1}$
infrared absorption coefficient,	$30\,mm^{-1}$
heat loss coefficient at the skin-air boundary	$10\,W\,m^{-2}K^{-1}$

Table 1: Tissue parameter values[9] used to generate three-dimensional thermal point spread function K_T.

3 METHODS

A program employing a non-negative constrained conjugate-gradient algorithm to solve Eq. 1 has been implemented on a DEC Alpha 3000 computer. In this technique, the initial estimate for ΔT^{3D} is taken to be zero, and adjusted at successive iterations to minimize the difference between the simulated time sequence of infrared emission images and that computed from Eq. 1. The algorithm is constrained so that negative values of ΔT^{3D} are not permitted.

Three simulated rectangular parallelpiped blood vessels ($60\times60\times600\,\mu m^3$), lateral separation $300\,\mu m$, depth $250\,\mu m$, were positioned in a $1\times1\times0.75\,mm^3$ volume of skin. The three-dimensional temperature increase in skin immediately following pulsed laser irradiation, ΔT^{3D}, was stored in a 64×64×64 element array in the computer, where each element represents a voxel of the simulated skin volume (Fig. 1). Light absorption in the epidermis was neglected. Infrared emission images of the skin surface at 64 uniformly spaced time points in the interval (0,0.42] s was used as input to the conjugate-gradient algorithm. The algorithm does not require any particular geometry, but this model was selected to simplify our analysis.

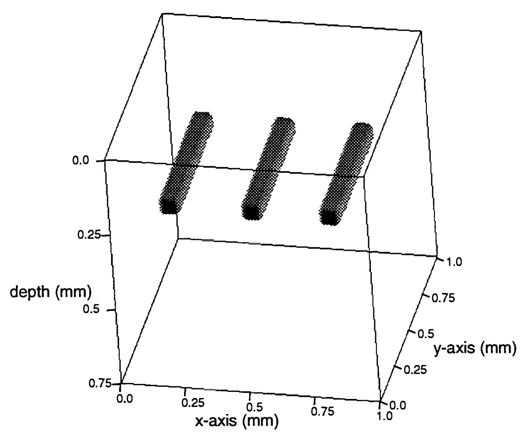

Figure 1: The position of vessels in skin model and coordinate system used.

The computed image simulates results from an IR-FPA camera operating in "snapshot mode", where all pixels are active at the same time. For this technique to be used with cameras that operate in "rolling readout" mode, additional processing is required to assign a varying time offset to the data from each pixel in the IR-FPA.

4 RESULTS

Initial result after 50 iterations of the constrained conjugate-gradient program are shown in Fig. 2, which required one hour of CPU time on a DEC Alpha 3000 computer. From Fig. 2a and 2b, depth and lateral position of the three vessels is predicted correctly but the cross-sectional vessel area has increased.

These results are encouraging as they show the potential of the IRT technique. Additional simulations are required to analyze the effect of the parameters in the simulation.

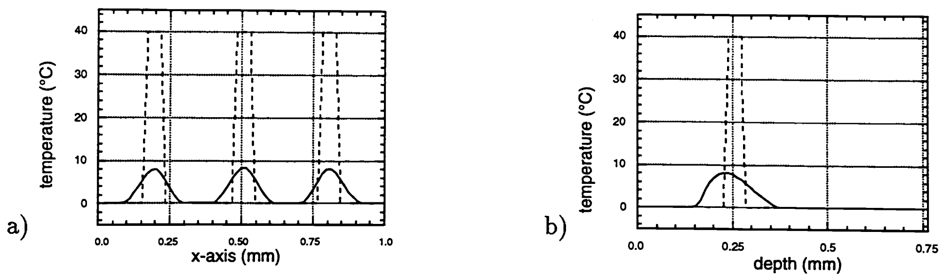

Figure 2: The temperature along the lines $y = 0.5\,\mathrm{mm}$, $z = 0.25\,\mathrm{mm}$ (a) and $x = 0.5\,\mathrm{mm}$, $y = 0.5\,\mathrm{mm}$ (b) in the arrays containing the computed (----) and true (—–) value of ΔT^{3D}.

5 CONCLUSIONS

Our simulation shows that the depth and lateral position of PWS vessels can be predicted from the time sequence of recorded infrared emission images. For this simulation, the vessel diameter is overestimated but underestimates the peak temperature.

6 ACKNOWLEDGEMENTS

This project was supported by research grants awarded from the Biomedical Research Technology Program (R03-RR06988) and Institute of Arthritis and Musculoskeletal and Sin Diseases (1R29-AR41638-01A1 and 1R01-AR42437-01A1) at the National Institutes of Health, Whitaker Foundation (TEM), and Dermatology Foundation. Institutional support from the Office of Naval Research, Department of Energy, National Institutes of Health, and the Beckman Laser Institute and Medical Clinic Endowment is also gratefully acknowledged. Work of Dennis Goodman was performed under the auspices of a U. S. Department of Energy grant to the Lawrence Livermore National Laboratory under Contract W-7405-Eng-48.

7 REFERENCES

1. A. H Jacobs and R. G Walton. "The incidence of birthmarks in the neonate", *Pediatrics*, 58, pp 218–22, 1976.
2. O. T Tan, S Murray, and A. K Kurban. "Action spectrum of vascular specific injury using pulsed irradiation", *Journal of Investigative Dermatology*, 92, pp 868–71, 1989.
3. J. W Pickering, P. H Butler, B. J Ring, and E. P Walker. "Computed temperature distributions around ectatic capillaries exposed to yellow (578 nm) laser light", *Physics in Medicine and Biology*, 34, pp 1247–58, 1989.
4. J. W Pickering, P. H Butler, B. J Ring, and E. P Walker. "Thermal profiles of blood vessels heated by a laser", *Australasian Physical & Engineering Sciences in Medicine*, 12, pp 11–5, 1989.
5. S Kimel, L. O Svaasand, M Hammer-Wilson, M. J Schell, T. E Milner, J. S Nelson, and M. W Berns. "Differential vascular response to laser photothermolysis", *Journal of Investigative Dermatology*, 103, pp 693–700, 1994.
6. T. E Milner, D. M Goodman, B. S Tanenbaum, and J. S Nelson. "Depth profiling of laser-heated chromophores in biological tissues by pulsed photothermal radiometry", *Journal of the Optical Society of America A*, 12, pp 1479–88, 1995.
7. T. E Milner, D. M Goodman, B. S Tanenbaum, B Anvari, L. O Svaasand, and J. S Nelson. "Imaging laser heated subsurface chromophores in biological materials: determination of lateral physical dimensions", *Physics in Medicine and Biology*, 41, pp 31–44, 1995.
8. M. J. C van Gemert, A. J Welch, I. D Miller, and O. T Tan. "Can physical modelling lead to an optimal laser treatment strategy for portwine stains?". In M. L Wolbarsht, editor, *Laser Applications in Medicine and Biology*, Vol. 5. Plenum Press, New York, 1991.
9. F. A Duck. *Physical Properties of Tissue: A Comprehensive Reference Book.* Academic Press, London, 1990.